Scientia Iranica F (2019) 26(6), 3896–3904

SCIENTIA
IRANICA

Sharif University of Technology
Scientia Iranica
Transactions F: Nanotechnology
http://scientiairanica.sharif.edu

Fast and clean dielectric barrier discharge plasma functionalization of carbon nanotubes decorated by electrodeposited nickel oxide: Application to glucose biosensors

A.A. Khodadadi[a], **Y. Mortazavi**[b], and **M. Vesali-Naseh**[c,*]

a. *Catalysis and Nanostructured Laboratory, School of Chemical Engineering, University of Tehran, Tehran, Iran.*
b. *Nanoelectronics Centre of Excellence, University of Tehran, Tehran, P.O. Box 11365-4563, Iran.*
c. *Department of Chemical Engineering, Hamedan University of Technology, Hamedan, 65155, Iran.*

Received 18 September 2018; received in revised form 19 April 2019; accepted 28 May 2019

KEYWORDS
Plasma;
Functional;
Carbon nanotubes;
Nickel;
Biosensor.

Abstract. In this study, multi-walled carbon nanotubes (MWCNTs) were functionalized through dielectric-barrier-discharge plasma in the presence of the H_2O-saturated atmosphere at 70°C and atmospheric pressure. The functionalized MWCNTs (F-CNTs) were decorated with 10 nm electrochemically deposited nanoparticles of NiO followed by glucose oxidase (GOx) immobilization, and the treated electrode was used for glucose detection. TEM, FE-SEM, TPD, and XPS techniques were used to characterize NiO/F-CNTs samples. The maximum extent of oxygen-containing functional groups, including carbonyl, hydroxyl, and carboxylic groups, formed in the plasma contact time of 4 min. The optimum time for the chronoamperometric deposition of NiO was 3 min. The presence of GOx on the NiO/F-CNTs electrode displayed a quasi-reversible and surface-controlled reduction-oxidation wave at -0.52 V. The peak separation of this wave is 0.05 V. The GOx/NiO/F-CNTs electrode showed a linear performance at a glucose concentration of 0.2-3.8 mM with a sensitivity rate of 2.16 μA/mM and a detection limit of 93.0 μM.

1. Introduction

Hybrids of carbon nanotubes (CNTs) and metal oxide nanoparticles (NPs) or polymeric materials have received particular attention for their potential applications in various devices such as ion batteries [1], fuel cells [2], medical instrument [3,4], tissue engineering [5], and biosensors [6]. Glucose biosensors have remained the most attractive in terms of their significance in different applications including clinical detection, food industries, and environmental protection [7,8]. Many approaches including fluorescent spectroscopy [9], colorimetry [10], conductometry [11], and electrochemical [12,13] methods have improved for glucose monitoring. These techniques mostly rely on the detection of hydrogen peroxide, generated through the reaction of glucose oxidase (GOx) and glucose [14]. The electrochemical biosensors have been frequently used due to their high sensitivity and selectivity, simplicity, and low cost [13,15].

In spite of the exceptional properties of CNTs, the inherent hydrophobic surface hinders their dispersion in aqueous solutions. The functionalization of nanotubes with hydrophilic groups improves their interaction with solvent matrices and enhances their abilities

---

*. *Corresponding author. Tel.: +98 81 38411406*
Fax: +98 81 38411520
E-mail addresses: khodadad@ut.ac.ir (A.A. Khodadadi); mortazav@ut.ac.ir (Y. Mortazavi); Masood.vesali@hut.ac.ir (M. Vesali-Naseh).

doi: 10.24200/sci.2019.51666.2302

to be used in different applications such as biological systems [16]. The connection of different functional species to the CNTs' surface can be achieved by using either wet chemical or dry oxidation approaches. The later method including plasma functionalization is a fast, flexible and non-polluting technique, which can create new active sites for enhancing the NP loadings and reducing their sizes on the surface of CNTs. Dielectric Barrier Discharge (DBD) is low-temperature and atmospheric pressure plasma, which can produce a uniform discharge atmosphere. The quantity of functional groups and surface defects may be controlled by power and exposure time of the plasma [16-17].

Among the various metal (oxide) NPs utilized in combination with CNTs, NiO with a small bandgap [18] has acquired special interest due to its ion exchange, molecular adsorption, environmental friendliness, and catalytic and electrochemical properties [19,20]. In addition, nickel can be combined with other metals, such as cobalt and copper, to enhance the electrochemical and catalytic properties of the biosensor electrode [21-22]. To the best of the author's knowledge, the composition of NiO and CNTs was rarely utilized for analytical glucose detection. One of the promising methods for fabricating CNT-NiO hybrid is the electrochemical deposition approach, by which the thickness of NiO film might be controlled through regulating parameters of the electrochemical process [23].

In the present work, multi-walled carbon nanotubes (MWCNTs) are functionalized through DBD plasma in the H_2O-saturated atmosphere at 70°C for 4 min. Afterwards, NiO-NPs are decorated on the MWCNTs' surface by an electrodeposition method. Finally, the glucose sensor is constructed using GOx immobilization on the surface of NiO/F-CNTs and is utilized in glucose detection experiments.

2. Materials and methods

2.1. Reagents

GOx (EC 1.1.3.4) and MWCNTs were purchased from Sigma-Aldrich and Shenzhen Nanotech Co. Ltd., respectively. All other reagents are of analytical grade, obtained from Merck. The phosphate buffer solution (PBS, KH_2PO_4 + K_2HPO_4) and the other solution samples were made using deionized water at pH 7.0.

2.2. Equipment

The electrochemical studies were performed through the typical three-electrode cells that include Pt as a counter electrode, a working Glassy Carbon Electrode (GCE, $A = 3.14 \times 10^{-2}$ cm^2), and Ag/AgCl as a reference electrode. The experiments were carried out in ambient conditions. The structure, morphology, and oxygenated groups of the nanotube hybrids were examined by Transmission Electron Microscopy (TEM) equipped with energy dispersive X-ray spectroscopy (EDS), Field Emission Scanning Electron Microscopy (FE-SEM), X-ray Photoelectron Spectroscopy (XPS), and Fourier transformed infrared spectroscopy (FTIR). The Temperature-Programmed Desorption (TPD) was performed for quantitative analyses of the functional groups of plasma-functionalized MWCNTs. This method was explained in another research work of ours [12].

2.3. DBD plasma functionalization of MWCNTs

In order to remove surface groups that are possibly produced via synthesis or purification period, the purchased MWCNTs were annealed at high temperatures (1000°C) in He. The process of functionalization (Figure 1(a)) was done through DBD in saturated air. The zero air with a flow rate of 40.0 sccm was humidified using H_2O at 70°C and moved over the

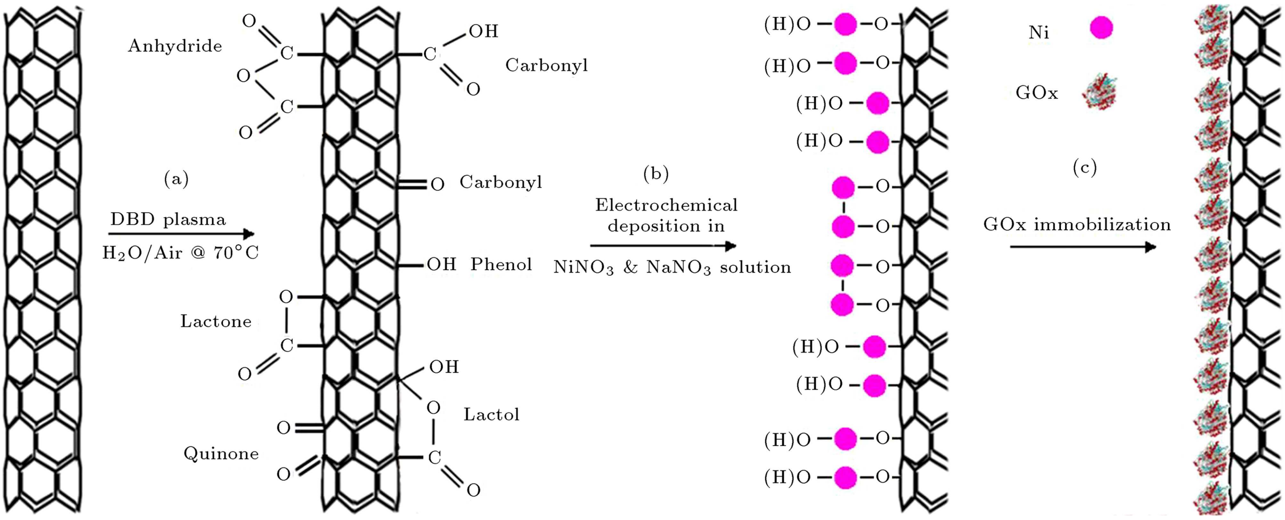

Figure 1. The process steps of GOx/NiO/F-CNTs/GC electrode fabrication for analytical glucose detection.

annealed MWCNTs inside a plasma reactor. The details of the reactor were given elsewhere [16]. The nanotube samples were exposed to DBD plasma at various times (i.e., 1, 2, 4, and 6 min). In this text, the DBD functionalized nanotubes are called F-CNTs.

2.4. Preparation of electrodes

The unmodified electrode was cleaned using polishing tissue and alumina slurry and was sonicated in the ethanol/water mixture. The F-CNTs were dissolved in nafion solution (0.5 wt.%) and mixed for 10 min using an ultrasonic homogenizer (250 UL Hielscher) to obtain uniform suspension (2.0 mg/ml). Then, 10.0 μl of this mixture was cast on the surface of GCE and dried at 25°C. To fabricate the NiO/F-CNTs/GCE (Figure (1)b), F-CNTs/GCE was inserted in the solution of $NiNO_3/NaNO_3$ (0.005 M) at constant potential (i.e., −0.8 V), versus reference electrode, for 3 min and rinsed in water. Subsequently, 5.0 μL of the GOx solution at a concentration of 10.0 mg/ml was immobilized on the surface of NiO/F-CNTs/GCE (Figure 1(c)) and dried at 4°C overnight. A concentration range of 0.01-4.0 mM glucose was selected for glucose detection experiments. The GOx/NiO/F-CNTs/GCE was stored at 4°C in the refrigerator.

3. Results and discussion

3.1. Characterization

3.1.1. TPD analyses of F-CNTs

Figure 2 presents TPD profiles of F-CNTs samples functionalized in the humid air for different exposure times. The gas evolution profile starts from 160°C and shows three major peaks at around 250, 400, and 800°C. These evolved gases that mainly include H_2O, CO_2, and CO result from the decomposition of oxygenated functional groups [24]. The area at the peaks of TPD spectrum (Figure 2 inset) corresponds to the total amount of the evolved gases. As the exposure time increases from 1 to 4 min, the amount of evolved gases is enhanced. An additional exposure time of 6 min results in a smaller quantity of functional groups. Since there is a limited number of defect points on the surface of nanotubes, as the primary site for functionalization, further plasma treatment leads to the detachment of some of the functional groups [25]. Figure 2(b) shows the TPD profile of MWCNTs functionalized for 4 min, which is deconvoluted to 5 peaks corresponding to H_2O, CO_2, and CO evolution during the decomposition of various oxygenated functional groups including carboxylic, anhydride, phenol, lactone, carbonyl, and quinone groups.

In order to evaluate the emerged gases, the TPD instrument was coupled with an FTIR gas cell, and the results of the identified and quantified evolved gases at various temperatures are shown in Figure 3. The major component in the low-temperature region of 160-280°C is H_2O, which is originated either from water trapped in the micropores or from the interaction of adjacent OH-containing groups [26]. The decomposition of these functional groups leads to the formation of carboxylic anhydrides and H_2O molecules [27].

The intermediate temperature region in the range of 260-600°C is mostly a mixture of H_2O and CO_2. These gases have evolved from the dissociation of phenol and carboxylic/anhydride groups [27,28]. The

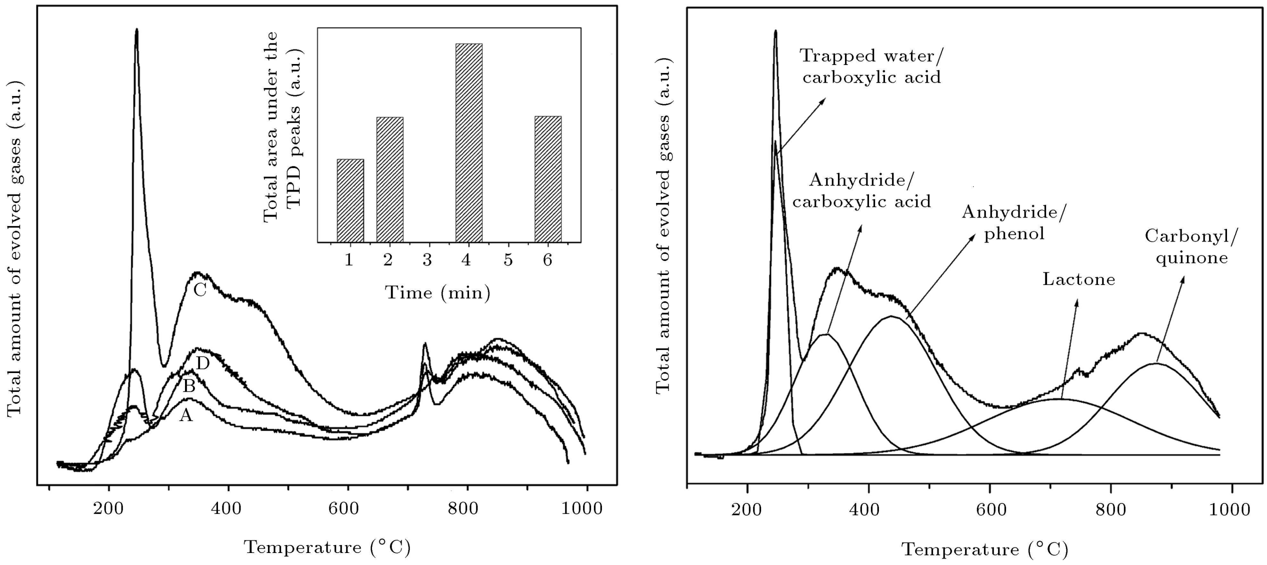

(a) (b)

Figure 2. (a) TPD spectra of MWCNTs functionalized at power = 30.6 W and various exposure times of (A) 1, (B) 2, (C) 4, and (D) 6 min. Inset: the influence of contact time on the total amount of evolved gases. (b) Deconvoluted peaks of TPD profile of MWCNTs functionalized for 4 min corresponding to different functional groups.

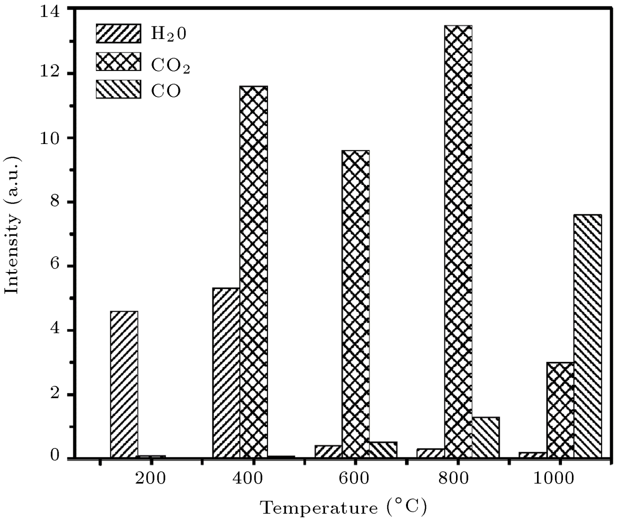

Figure 3. The relative amounts of evolved H_2O, CO, and CO_2 from the MWCNTs functionalized in the DBD plasma for 4 min at various temperatures during the TPD experiment.

slight CO evolution around 600°C results from the decomposition of anhydride and phenol groups [28]. The high-temperature region of 600-1000°C is mainly attributed to the evolution of CO_2 and CO from lactone and carbonyl/quinone groups, respectively [28]. The existence of these oxygenated functional groups on the F-CNTs' surface was confirmed by FTIR in our other work [12]. Another major source of CO_2 desorption in the high-temperature region is the secondary reaction between CO and oxygen surface species, as shown in the following:

$$CO + C - O \rightarrow CO_2 + C_a, \qquad (1)$$

where C_a is the adsorption site on the CNTs' surface, and C-O is the oxygenated group attached to the nanotubes. During the TPD, C_a may also react with the desorbed H_2O, CO_2, and CO and reform the oxygenated functional groups.

3.1.2. XPS results

To further study the surface chemical state of different F-CNTs samples, XPS survey spectra were employed. The XPS data for the annealed sample and F-CNTs (Figure 4(a)) indicate the presence of carbon and oxygen atoms. During the DBD plasma treatment of MWCNTs, the photoelectron peak of O 1s at 533 eV increases from 1.5% to 5.6% for the annealed and functionalized samples, respectively. In order to examine the bond structure of the oxygen-containing species, the C 1s peak was deconvoluted, the results of which are presented in Figure 4(a), inset. The major component at 284.9 eV is attributed to C=C bond, and the peaks at 286.3, 287.2, and 288.4 eV can be assigned to hydroxyl, carbonyl, and carboxyl groups, respectively [29]. These oxygenated species are created through the interaction of the reactive components such as O, O_3, H, and OH with the surface of MWCNTs. These reactive species generated during DBD plasma in humid air atmosphere can split C=C bond and interact with open ends and defect points of CNTs [16]. The oxygenated groups have polar properties and make negative charges on the surface of CNTs and improve dispersion in aqueous solutions [12].

Figure 4(b) illustrates XPS spectra of NiO/F-CNT sample. The attachment of nickel oxide to the surface of F-CNTs leads to increasing the percentage of oxygen atoms to 11.3%. Two photoelectron peaks

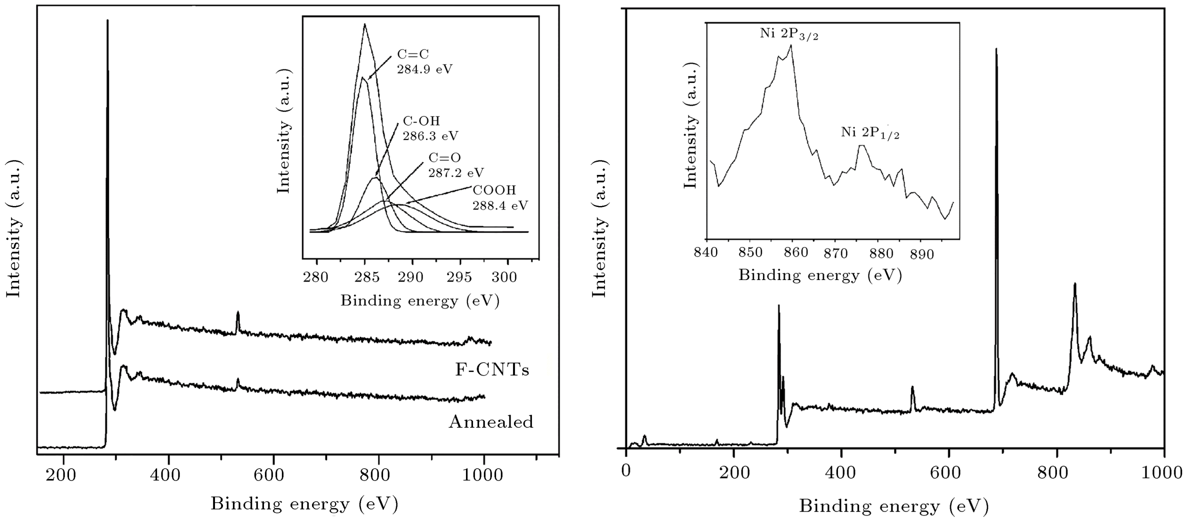

(a)

(b)

Figure 4. (a) The XPS spectra of the annealed sample and F-CNTs. Inset: deconvolution of C 1s XPS spectra of F-CNTs. (b) XPS spectra of NiO/F-CNTs. Inset: the magnified region of Ni 2p: The peaks at 857.7 and 875.7 eV were attributed to Ni $2p_{3/2}$ and Ni $2p_{1/2}$, respectively.

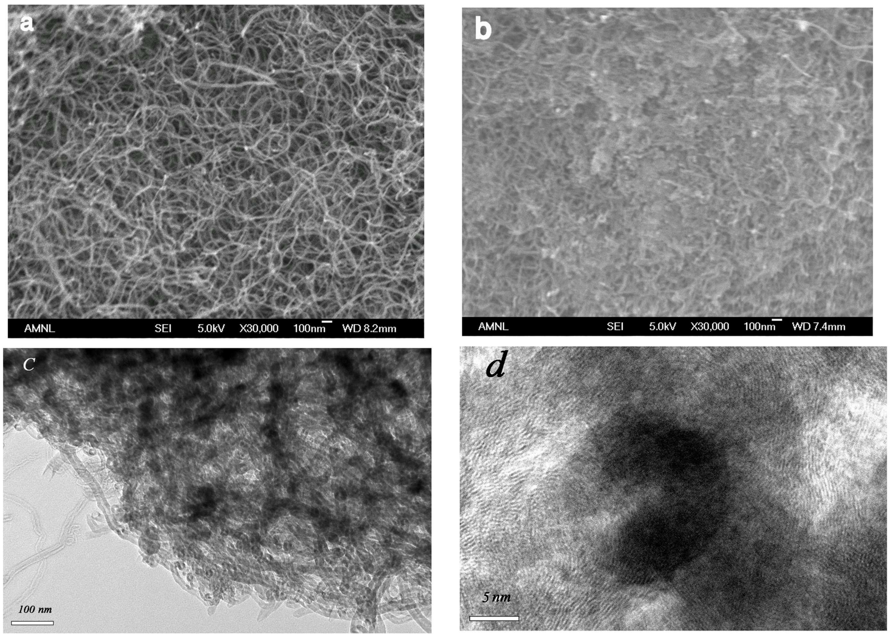

Figure 5. The SEM micrographs of (a) F-CNTs and (b) NiO/F-CNTs. (c) TEM image and (d) HRTEM of NiO/F-CNTs hybrid.

at 857.7 and 875.7 eV might be related to $Ni2p_{3/2}$ and $Ni2p_{1/2}$, respectively [30]. Moreover, the percentage of Ni atoms in the NiO/F-CNT hybrid was calculated to be about 5.4%.

3.1.3. *Morphology of F-CNTs and NiO/F-CNTs*

The FE-SEM micrograph obtained for F-CNTs (Figure 5(a)) reveals a twisted morphology of MWCNTs with diameters of 20-30 nm, while the length reaches tens of micrometers. The SEM of NiO/F-CNTs sample (Figure 5(b)) shows that NiO-NPs are deposited on the nanotubes' surface and a relatively thin film is created. The TEM image of NiO/F-CNTs (Figure 5(c)) further shows that NiO has uniformly and directly grown on the CNTs' surface. From the HRTEM image of the NiO/F-CNTs (Figure 5(d)), the particle size of NiO-NPs was determined to be approximately 10 nm. EDS analyses (data not shown here) confirm the presence of carbon, oxygen, and nickel elements in the NiO/F-CNTs hybrid.

3.2. **Biosensor performance**

3.2.1. *Optimum deposition time*

Figure 6 presents the cyclic voltammogram of NiO/F-CNTs electrodes synthesized by chronoamperometry at different deposition times. The formation of NiO-NPs (Eqs. (2)-(4)) [20] on the surface of F-CNTs/GCE increases current, indicating that the electroactive surface of NiO/F-CNTs/GC electrode is enhanced.

$$2OH^- + Ni^{2+} \rightarrow Ni(OH)_2, \qquad (2)$$

$$Ni(OH)_2 \rightarrow H_2O + NiO, \qquad (3)$$

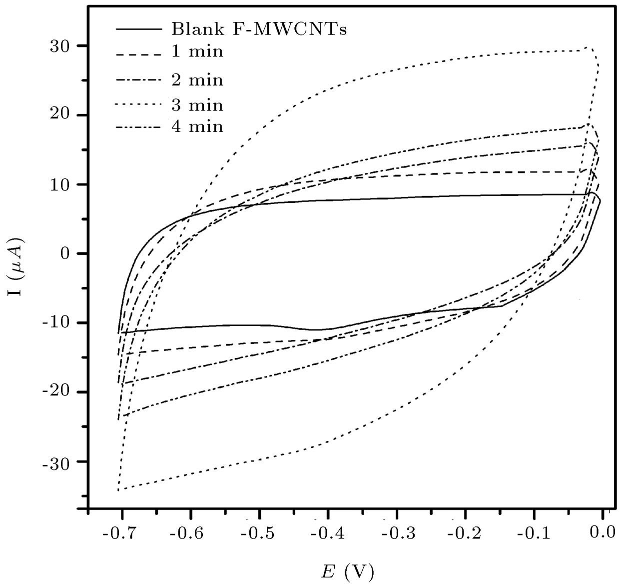

Figure 6. The cyclic voltammograms of blank F-CNTs and NiO/F-CNTs electrodes synthesized by the chronoamperometry method at different deposition times.

$$2C = O + 2Ni^{+2} \rightarrow 2C - NiO. \qquad (4)$$

The charging current improvement is the greatest for the optimum deposition time of 3 min, and a further increase in the deposition time may cause the agglomeration of NiO-NPs and the reduction of the reactive surface of the modified working electrode.

3.2.2. *Enzyme immobilization*

The modified electrodes were investigated using cyclic voltammetry in the range of −0.8-0 V, the results

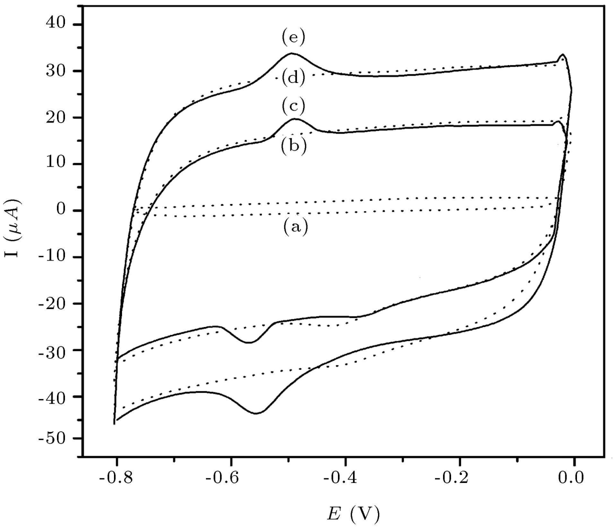

Figure 7. The cyclic voltammograms of (a) bare GCE, (b) F-CNTs/GCE, (c) GOx/F-CNTs/GCE, (d) NiO/F-CNTs/GCE, and (e) GOx/NiO/F-CNTs/GCE.

of which are illustrated in Figure 7. The anodic charging current has increased from 2.0 μA for the bare GCE (Figure 7(a)) to 15.0 μA for F-CNTs/GCE (Figure 7(b)), indicating that the functionalized nanotubes improve the reactive surface of treated electrodes. The GOx immobilization on the F-CNTs/GC electrode (Figure 7(c)) has created a reduction-oxidation wave centered at -0.54 V with a peak-to-peak potential separation (ΔE_p) of 0.08 V.

Because of the existence of NiO-NPs on the F-CNTs/GCE (Figure 7(d)), the reactive surface has further increased and enhanced the efficient points for the adsorption of GOx. The GOx/NiO/F-CNTs/GCE (Figure 7(e)) presents a reduction-oxidation wave at -0.52 V with ΔE_p of 0.05 V. The metal NPs may act as effective electron-conducting channels and decrease working potential and ΔE_p for the enzymatic electrode. The modified electrodes in the absence of GOx show no faradic current as a result of the oxidation-reduction process, suggesting that the reduction-oxidation activity of the modified electrodes is assigned to the immobilized GOx as follows:

$$\mathrm{GOx(FAD)} + 2\mathrm{e} + 2\mathrm{H}^+ \leftrightarrow \mathrm{GOx(FADH_2)}. \qquad (5)$$

3.2.3. Effect of the scan rate

The effect of various scan rates on the cyclic voltammograms of GOx/NiO/F-CNTs electrodes is presented in Figure 8. ΔE_p of GOx peaks has slightly increased with an increase in the scan rate. Moreover, the currents of cathodic and anodic peaks are closely equal and show linear behavior ($R^2 = 0.99$) versus the scan rate in the range of 10-250 mV/s. The results (Figure 8(b)) illustrate that the reduction-oxidation process is quasi reversible and surface confined [31].

The plots of cathodic and anodic potential peak (E_p) versus the log of scan rate are given in Figure 8(c). As shown, at a scan rate of 80 to 250 mV/s, two lines with the slopes of $\pm 2.3RT/\alpha nF$ are generated. In this equation, α is the coefficient of charge transfer, n is the number of transferred electrons, and other parameters are constant ($T = 298$ K, $R = 8.314$ J/mol.K, $F = 96485$). Through the slope of plotted lines, the mean values of α and n were approximated to be 0.39 and 2, respectively. In addition, the charge transfer rate constant (k_s) of the enzyme at a scan rate of 250 mV/s was evaluated to be 1.12 ± 0.1 s^{-1} based on Laviron's equation [32]:

$$\log k_s = \alpha \log(1-\alpha) + (1-\alpha)\log\alpha - \log(\frac{RT}{nF\nu}) - \alpha(1-\alpha)\frac{nF\Delta E_p}{2.3RT}. \qquad (6)$$

The average GOx concentration (Γ) was calculated through the following equation:

$$I_p = (\frac{n^2F^2A\Gamma}{4RT})\nu, \qquad (7)$$

where A denotes the surface area of the treated electrode (0.125 cm^2), and I_p is the peak current. Through the slope of plot of peak currents versus scan rate (Figure 8(b)), the GOx concentration was calculated to be 1.2×10^{-9} mol/cm^2. In addition, the ratio of GOx/NiO was estimated to be about 5.4, suggesting that the multi-layered GOx was involved in the process of electron transferring.

3.2.4. Glucose detection using GOx/NiO/F-CNTs/GCE

The response of GOx/NiO/F-CNTs/GCE toward the addition of glucose was studied using cyclic voltammetry [33,34], the results of which are shown in Figure 9. The oxidation current decreases from 19.8 to 11.0 μA with a sequential glucose addition due to the blocking effect of the modified electrode [28]. The reaction mechanism of glucose in the sensor matrix was proposed to be [13]:

$$\mathrm{Glucose} + \mathrm{GOx(FAD)} \rightarrow \mathrm{Gluconolactone} + \mathrm{GOx(FADH_2)}, \qquad (8)$$

$$2\mathrm{NiO} + 2\mathrm{H_2O_2} \rightarrow 2\mathrm{Ni(OH)_2} + \mathrm{O_2}, \qquad (9)$$

$$2\mathrm{OH}^- + 2\mathrm{Ni(OH)_2} \leftrightarrow 2\mathrm{H_2O} + 2\mathrm{NiO(OH)} + 2\mathrm{e}^-, \qquad (10)$$

$$\mathrm{GOx(FADH_2)} + 2\mathrm{NiO(OH)} \rightarrow \mathrm{GOx(FAD)} + 2\mathrm{NiO} + 2\mathrm{H_2O}. \qquad (11)$$

Figure 9, inset, presents the corresponding curve of calibration based on anodic faradic current response. The current response in the range of 0.2-3.8 mM presents a linear performance with the equation of:

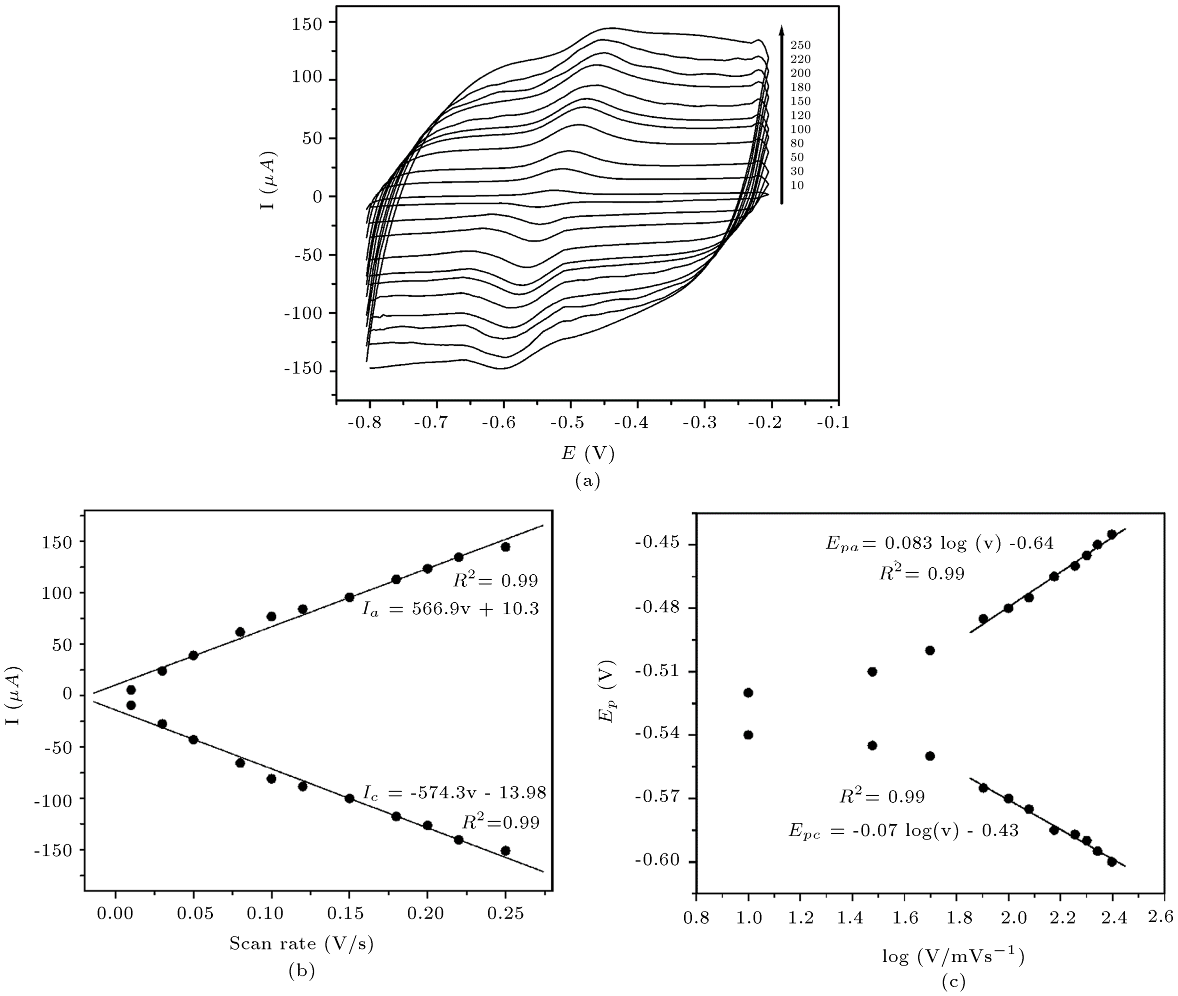

(a)

(b)

(c)

Figure 8. (a) The cyclic voltammograms of GOx/NiO/F-CNTs/GCE in 0.1 M PBS at various scan rates of 10-250 mV/s. (b) The peak current plot versus scan rate. (c) The plot of E_p versus log (scan rate).

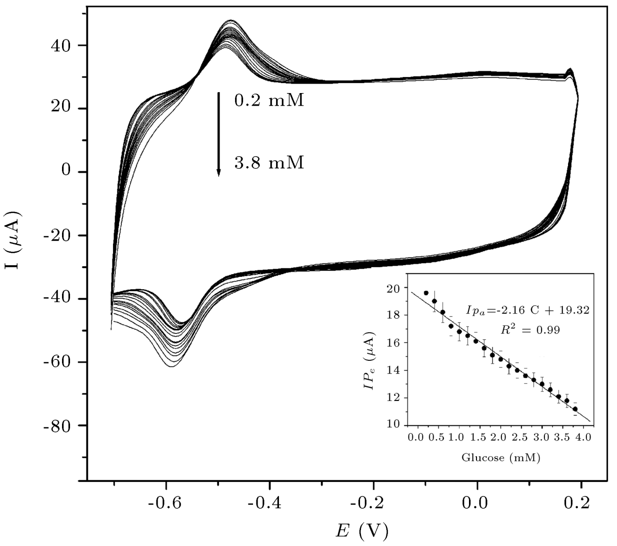

Figure 9. Cyclic voltammograms of the GOx/NiO/F-CNTs/GCE in the presence of 0.2 (outer) to 3.8 mM (inner) glucose. Inset: the curve of calibration for oxidation currents at different glucose concentrations.

$$I(\mu A) = -2.16\text{C (mM)} + 19.32 \ (R^2 = 0.99).$$

The modified electrode shows relatively high sensitivity of 2.16 μA/mM that may be assigned to the high surface area of F-CNTs and high electro-catalytic activity and adsorption ability of NiO-NPs. The detection limit of the fabricated electrode was estimated to be 93.0 μM based on a signal-to-noise ratio of 3. Table 1 reports the analytical characteristics of the GOx/NiO/F-CNTs/GCE. This result is comparable to other works that have utilized nickel oxide in the medium of immobilization. It is noted that the electrode preparation process in the present work is fairly faster and simpler than that of other reports.

4. Conclusions

GOx/NiO/F-CNTs modified electrodes for glucose detection were fabricated by the treatment of nanotubes in the DBD plasma reactor in humid air, followed by electrodeposition of NiO and immobilization of GOx.

Table 1. The comparison of GOx/NiO/F-CNTs/GCE and other similar electrodes.

Electrode material	Formal potential (V)	Sensitivity (μA.mM $^{-1}$)	Detection limit (μM)	Linear range (mM)	Ref.
GOx/NiO/GC	−0.42	0.44	24	0.03-5	[34]
CHIT[a] /GOx/NiO/GC	0.35	3.43	47	1.5-7	[19]
NiCFP[b] electrode	0.6	3.3	1	0.002-2.5	[7]
GOx/NiO/F-CNTs/GCE	-0.52	2.16	93	0.2-3.8	This work

[a] Chitosan; [b] Carbon nanofiber paste.

The functionalization increased the oxygen-containing groups of MWCNTs from 1.5 to 5.6%, which in turn led to an important improvement of the anodic charging current. The larger number of oxygenated groups rolled as active centers for the uniform decoration of the F-CNTs with 10 nm NiO-NPs. This decoration improved the electroactive surface area and enhanced the immobilization of GOx by electrostatic attraction on the basic NiO. The presence of NiO-NPs improved electron transfer efficiency and reversibility of GOx reduction-oxidation wave, which is a quasi-reversible and surface-confined process.

References

1. Ren, J., Wang, Z., Yang, F., Ren, R.P., and Lv, Y.K. "Freestanding 3D single-wall carbon nanotubes/WS_2 nanosheets foams as ultra-long-life anodes for rechargeable lithium ion batteries", *Electrochimica. Acta*, **267**, pp. 133-140 (2018).
2. Huang, J., Zhu, N., Yang, T., Zhang, T., Wu, P., and Dang, Z. "Nickel oxide and carbon nanotube composite (NiO/CNT) as a novel cathode non-precious metal catalyst in microbial fuel cells", *Biosens. Bioelectron.*, **72**, pp. 332-339 (2015).
3. Amirian, M., Nabipour Chakoli, A., Cai, W., and Sui, J. "Effect of functionalized multiwalled carbon nanotubes on thermal stability of poly (L-LACTIDE) biodegradable polymer", *Sci. Iran*, **20**, pp. 1023-1027 (2013).
4. Foroughi, M.R., Khoroushi, M., Nazem, R., and Akbarian Tefaghi, E. "The effect of carbon nanotubes/bioglass nanocomposite on mechanical and bioactivity properties of glass ionomer cement", *Sci. Iran*, **23**, pp. 3123-3134 (2016).
5. Karbasi, S., Zarei, M., and Foroughi, M.R. "Effect of multi-wall carbon nanotubes (MWNTs) on structural and mechanical properties of poly(3-hydroxybutirate) electrospun scaffolds for tissue engineering applications", *Sci. Iran*, **23**, pp. 3145-3152 (2016).
6. Si, P., Huang, Y., Wang, T., and Ma, J. "Nanomaterials for electrochemical non-enzymatic glucose biosensors", *RSC Adv.*, **3**, pp. 3487-3502 (2013).
7. Liu, Y., Teng, H., Hou, H., and You, T. "Nonenzymatic glucose sensor based on renewable electrospun Ni nanoparticle-loaded carbon nanofiber paste electrode", *Biosens. Bioelectron.*, **24**, pp. 3329-3334 (2009).
8. Qian, Q., Hu, Q., Li, L., Shi, P., Zhou, J., Kong, J., Zhang, X., Sun, G., and Huang, W. "Sensitive fiber microelectrode made of nickel hydroxide nanosheets embedded in highly-aligned carbon nanotube scaffold for nonenzymatic glucose determination", *Sens. Actuators*, **257**, pp. 23-28 (2018).
9. Barrio, M., Moros, M., Puertas, S., Fuente, J.M., Grazú, V., Cebolla, V., Marcos, S., and Galbán, J. "Glucose oxidase immobilized on magnetic nanoparticles: Nanobiosensors for fluorescent glucose monitoring", *Microchim. Acta*, **184**, pp. 1325-1333 (2017).
10. Pang, Y., Huang, Z., Yang, Y., Long, Y, and Zheng, H. "Colorimetric detection of glucose based on ficin with peroxidase-like activity", *Spectrochim. Acta A Mol. Biomol. Spectrosc.*, **189**, pp. 510-515 (2018).
11. Miwa, Y., Nishizawa, M., Matsue, T., and Uchida, I. "A conductometric glucose sensor based on a twin-microband electrode coated with a polyaniline thin film", *Bull. Chem. Soc. Jpn.*, **67**, pp. 2864-2866 (1994).
12. Vesali-Naseh, M., Khodadadi, A.A., Mortazavi, Y., Moosavi-Movahedi, A.A., and Ostrikov, K. "H_2O/air plasma-functionalized carbon nanotubes decorated with MnO_2 for glucose sensing", *RSC Adv.*, **6**, pp. 31807-31815 (2016).
13. Mathew, M., and Sandhyarani, N. "A highly sensitive electrochemical glucose sensor structuring with nickel hydroxide and enzyme glucose oxidase", *Electrochim. Acta.*, **108**, pp. 274-280 (2013).
14. Gao, F., Yin, J., Yao, Z., Li, M., and Wang, L. "A nanocomposite modified electrode: electrocatalytic properties and its sensing applications to hydrogen peroxide and glucose", *J. Electrochem. Soc.*, **157**, pp. F35-F39 (2010).
15. Gorgin Karaji, Z., Houshmand, B., Abbasi, S., and Faghihi, S. "Electrochemical anodic oxidation process of porous titanium granules for biomedical applications", *Sci. Iran*, **22**, pp. 2745-2751 (2015).
16. Vesali-Naseh, M., Khodadadi, A.A., Mortazavi, Y., Pourfayaz, F., Alizadeh, O., and Maghrebi, M. "Fast and clean functionalization of carbon nanotubes by dielectric barrier discharge plasma in air compared to acid treatment", *Carbon*, **48**, pp. 1369-1379 (2010).
17. Zhang, H., Li, H., Fang, M., Wang, Z., Sang, L., Yang, L., and Chen, Q. "Roll-to-roll DBD plasma pretreated polyethylene web for enhancement of Al coating adhesion and barrier property", *Appl. Surf. Sci.*, **388**, pp. 539-545 (2015).

18. Abdi, M.H., Ibrahim, N.B., Baqiah, H., and Halim, S.A. "Structural, electrical and magnetic characterization of nickel-doped tin oxide film by a sol-gel method", *Sci. Iran*, **21**, pp. 2459-2467 (2014).
19. Li, C., Liu, Y., Li, L., Du, Z., Xu, S., Zhang, M., Yin, X., and Wang, T. "A novel amperometric biosensor based on NiO hollow nanospheres for biosensing glucose", *Talanta*, **77**, pp. 455-459 (2008).
20. Yao, M., Hu, Z., Xu, Z., Liu, Y., Liu, P., and Zhang, Q. "High-performance electrode materials of hierarchical mesoporous nickel oxide ultrathin nanosheets derived from self-assembled scroll-like a-nickel hydroxide", *J. Power Sour.*, **273**, pp. 914-922 (2015).
21. Ammara, S., Shamaila, S., Zafar, N., Bokhari, A., and Sabah, A. "Nonenzymatic glucose sensor with high performance electrodeposited nickel/copper/carbon nanotubes nanocomposite electrode", *J. Phys. Chem. Solids.*, **120**, pp. 12-19 (2019).
22. Ko, T.H., Seong, J.G., Radhakrishnan, S., Kwak, C.S., Khil, M.S., Kim, H.Y., and Kim, B.S. "Dual functional nickel cobalt/MWCNT composite electrode-based electrochemical capacitor and enzymeless glucose biosensor applications: Influence of Ni/Co molar ratio", *J. Ind. Eng. Chem.*, **73**, pp. 1-7 (2019).
23. Xu, J.J., Feng, J.J., Zhong, X., and Chen, H.Y. "Low-potential detection of glucose with a biosensor based on the immobilization of glucose oxidase on polymer/manganese oxide layered nanocomposite", *Electroanal.*, **20**, pp. 507-512 (2008).
24. Chen, J., Kobayashi, F., Eguchi, K., and Waki, K. "Understanding the redox reactions of adjacent carboxyl groups and anhydride groups following citric acid treatment of defect-containing multiwalled carbon nanotubes", *Electrochem. Commun.*, **91**, pp. 25-30 (2018).
25. Xu, T., Yang, J., Liu, J., and Fu, Q. "Surface modification of multi-walled carbon nanotubes by O_2 plasma", *Appl. Surf. Sci.*, **253**, pp. 8945-89451 (2007).
26. Rosenthal, D., Ruta, M., Schlögl, R., and Kiwi- "Combined XPS and TPD study of oxygen-functionalized carbon nanofibers grown on sintered metal fibers", *Carbon*, **48**, pp. 1835-1843 (2010).
27. Boehm, H.P. "Surface oxides on carbon and their analysis: a critical assessment", *Carbon*, **40**, pp. 145-149 (2002).
28. Figueiredo, J.L. and Pereira, M.F. "The role of surface chemistry in catalysis with carbons", *Catal. Today*, **150**, pp. 2-7 (2010).
29. Tayyebi, A., Tavakoli, M.M., Outokesh, M., Shafiekhani, and A., Simchi, A. "Supercritical synthesis and characterization of graphene PbS Quantum dots composite with enhanced photovoltaic properties", *Ind. Eng. Chem. Res.*, **54**, pp. 7382-7392 (2015).
30. Hoa, L.T., Tien, H.N., Luan, V.H., Chung, J.S., and Hur, S.H. "Fabrication of a novel 2D-graphene/2D-NiO nanosheet-based hybrid nanostructure and its use in highly sensitive NO_2 sensors", *Sens. Actuators B*, **185**, pp. 701-705 (2013).
31. Mohammadi, F., Vesali-Naseh, M., Khodadadi A.A., and Mortazavi, Y. "A comparison of a nanostructured enzymeless Au/Fe_2O_3/MWCNTs/GCE electrode and a GOx modified one in electrocatalytic detection of glucose", *Electroanalysis*, **30**, pp. 1-10 (2018).
32. Haghighi, N., Hallaj, R., and Salimi, A. "Immobilization of glucose oxidase onto a novel platform based on modified TiO_2 and graphene oxide, direct electrochemistry, catalytic and photocatalytic activity", *Mater. Sci. Eng. C.*, **73**, pp. 417-424 (2017).
33. Li, F., Song, J., Li, F., Wang, X., Zhang, Q., Han, D., Ivaska, A., and Niu, L. "Direct electrochemistry of glucose oxidase and biosensing for glucose based on carbon nanotubes@SnO_2-Au composite", *Biosens. Bioelectron.*, **25**, pp. 883-888 (2009).
34. Salimi, A., Sharifi, E., Noorbakhsh, A., and Soltanian, S. "Immobilization of glucose oxidase on electrodeposited nickel oxide nanoparticles: Direct electron transfer and electrocatalytic activity", *Biosens. Bioelectron.*, **22**, pp. 3146-3153 (2007).

Biographies

Abbas Ali Khodadadi received his MSc in Chemical Engineering from University of Tehran in 1986 and his PhD in Catalysis and Reaction Engineering from University of Waterloo, Canada in 1994. His research interests include nanostructured materials synthesis, surface functionalization, characterization and use as (bio/photo/electro) catalysts, adsorbents, membranes in energy, environmental, chemicals production, and gas/bio-sensors applications.

Yadollah Mortazavi received the BSc degree in Chemical Engineering from University of Shiraz, Shiraz, Iran and the MSc and PhD degrees in Chemical Engineering from University of Waterloo, Waterloo, Ont., Canada. He joined University of Tehran, Tehran, Iran in 1995. His research interests include catalysis and reaction engineering, especially in C1 chemistry, environmental catalysis, chemical gas-sensors, and nano-structured materials. Currently, he is the Chair of Nanotechnology Department at College of Engineering, University of Tehran, Tehran, Iran.

Masoud Vesali-Naseh received MSc and PhD degrees from University of Tehran in 2009 and 2014, respectively. He is an Assistant Professor at the Chemical Engineering Department, University of Hamedan since 2014. His research interests are environmental issues, nanostructured materials, and catalytic reaction engineering.